Bose-Einstein condensation dynamics in three dimensions by the pseudospectral and finite-difference methods

Paulsamy Muruganandam†‡ **and Sadhan K Adhikari**†

†Instituto de Física Teórica, Universidade Estadual Paulista,
01.405-900 São Paulo, São Paulo, Brazil
‡ Centre for Nonlinear Dynamics, Department of Physics, Bharathidasan University,
Tiruchirapalli 620 024, Tamil Nadu, India

Abstract.
    We suggest a pseudospectral method for solving the three-dimensional time-dependent Gross-Pitaevskii (GP) equation and use it to study the resonance dynamics of a trapped Bose-Einstein condensate induced by a periodic variation in the atomic scattering length. When the frequency of oscillation of the scattering length is an even multiple of one of the trapping frequencies along the x, y, or z direction, the corresponding size of the condensate executes resonant oscillation. Using the concept of the differentiation matrix, the partial-differential GP equation is reduced to a set of coupled ordinary differential equations which is solved by a fourth-order adaptive step-size control Runge-Kutta method. The pseudospectral method is contrasted with the finite-difference method for the same problem, where the time evolution is performed by the Crank-Nicholson algorithm. The latter method is illustrated to be more suitable for a three-dimensional standing-wave optical-lattice trapping potential.

1. Introduction

The experimental realization [1] of Bose-Einstein condensates (BECs) in dilute weakly-interacting trapped bosonic atoms at ultra-low temperature initiated intense theoretical effort to describe the properties of the condensate [2, 3, 4, 5, 6, 7, 8, 9, 10, 11, 12, 13]. The properties of a condensate at zero temperature are usually described by the time-dependent, nonlinear, mean-field Gross-Pitaevskii (GP) equation [14]. The effect of the interatomic interaction leads to a nonlinear term in the GP equation which complicates the solution procedure. Also, to simulate the proper experimental situation one should be prepared to deal with an anisotropic trap [15].

A numerical study of the time-dependent GP equation is of interest, as this can provide solution to many stationary and time-evolution problems. The time-independent GP equation yields only the solution of stationary problems. As our principal interest is in time evolution problems, we shall only consider the time-dependent GP equation in this paper. There are many numerical methods for the solution of the GP equation [3, 4, 5, 6, 7, 8, 9, 10, 11, 12, 13].

Here we suggest a pseudospectral time-iteration method [16, 17] for the solution of the three-dimensional GP equation with an anisotropic harmonic trap and contrast it with the finite-difference method [18, 19]. In the pseudospectral method the unknown wave function is expanded in terms of a set of N orthogonal polynomials. When this expansion is substituted into the GP equation, the (space) differential operators operate on a set of known polynomials and generate a differentiation matrix operating on the unknown coefficients. Consequently, the time-dependent partial-differential nonlinear GP equation in space and time variables is reduced to a set of N coupled ordinary differential equations (ODEs) in time which is solved by a fourth-order adaptive step-size control Runge-Kutta method [20] using successive time iteration. In the pseudospectral method we use the Hermite polynomials to expand the wave function. In references [11] pseudospectral methods have been employed for the solution of the GP equation, where a variable step forth order Runge-Kutta time propagator was used, as in the present work. In [11] a pseudospectral fourier-sine basis was used for finite traps, and a corresponding complex pseudospectral basis was used for systems with periodic boundary conditions. However, the present study seems to be the first systematic study in dealing with the GP equation in three space dimensions using the pseudospectral and finite-difference approaches.

In the finite-difference method the time iteration is implemented by the split-step Crank-Nicholson scheme. The first approach will be termed pseudospectral-Runge-Kutta (PSRK) method and the second finite-difference-Crank-Nicholson (FDCN) method in the following. Here pseudospectral and finite-difference refer to the space part and Runge-Kutta and Crank-Nicholson refer to the time part. However, it should be noted that the temporal and the spatial parts in the GP equation can be dealt with in independent fashions. One can combine the pseudospectral or finite difference approach with a specific algorithm for time stepping which can be Runge-Kutta or Crank-Nicholson (with or without time-splitting) scheme, or any other. In fact it is quite common to implement some version of the pseudospectral method with Crank-Nicholson time stepping when solving the Navier-Stokes equation.

The PSRK method is illustrated by calculating the wave function and energy eigenvalue of the GP equation for different nonlinearity and trap symmetries in three dimensions as well as by studying a resonance dynamics. We find that in both cases the PSRK method presented here turns out to be a practical and efficient one for the solution of the time-dependent GP equation.

Resonance is an interesting feature of an oscillation under the action of an external periodic force manifesting in a large amplitude, when the frequency of the external force equals a multiple of the natural frequency of oscillation. Although, the phenomenon of resonance is well-understood in linear problems, in nonlinear dynamics it is far more nontrivial. Hence, it is worthwhile to study the dynamics of resonance using the nonlinear GP equation. The possibility of generating a resonance in a BEC subject to an oscillating trapping potential has been explored previously [21]. Here, using the PSRK approach we study the resonance dynamics of a three-dimensional BEC subject to a periodic variation in the scattering length. One can have resonant oscillation in the x, y, and z directions, when the frequency of oscillation of scattering length equals an even multiple of the trapping frequency in the respective direction. Such a variation in the scattering length is possible near a Feshbach resonance by manipulating an external magnetic field [22]. There have been recent studies on this topic in one [23] and two

space [24] variables.

Next we consider the FDCN method for the numerical solution of the time-dependent GP equation [4, 5, 6, 7, 8]. In this approach the time-dependent GP equation is first discretized in space and time using a specific rule [18, 19] and the resultant set of equations is solved by time iteration with an initial input solution [4, 5, 6, 7]. This procedure leads to good result in the effective one- [4] and two-space-variable [6, 5, 7, 8] cases and we extend it here to the full three-dimensional case. In the two-space-variable case a three-step procedure [8] is first used to separate the Hamiltonian into three parts before applying the Crank-Nicholson scheme in two directions. In the three-space variable case we consider a four-step procedure where the Hamiltonian is broken up into four parts. We illustrate the FDCN method in three dimensions for the solution of the GP equation with a three-dimensional standing-wave optical-lattice potential.

In section 2 we describe briefly the three-dimensional, time-dependent GP equation with an anisotropic trap. The PSRK and FDCN methods are described in section 3. In section 4 we report the numerical results for the wave function and energy for different symmetries and nonlinearities as well as an account of our study of resonance in the anisotropic case due to an oscillating scattering length. In section 5 we present the solution of the GP equation for an optical-lattice potential using the FDCN method and finally, in section 6 we present a discussion of our study.

2. Nonlinear Gross-Pitaevskii Equation

At zero temperature, the time-dependent Bose-Einstein condensate wave function $\Psi(\mathbf{r}; \tau)$ at position $\mathbf{r}$ and time τ may be described by the following mean-field nonlinear GP equation [2, 14]

$$\left[-\frac{\hbar^2 \nabla^2}{2m} + V(\mathbf{r}) + g N_0 |\Psi(\mathbf{r}; \tau)|^2 - i\hbar \frac{\partial}{\partial \tau} \right] \Psi(\mathbf{r}; \tau) = 0.$$

Here m is the mass and N_0 the number of atoms in the condensate, $g = 4\pi\hbar^2 a/m$ the strength of interatomic interaction, with a the atomic scattering length. The normalization condition of the wave function is $\int d\mathbf{r} |\Psi(\mathbf{r}; \tau)|^2 = 1$.

The three-dimensional trap potential is given by $V(\mathbf{r}) = \frac{1}{2}m(\omega_0^2 \bar{x}^2 + \omega_y^2 \bar{y}^2 + \omega_z^2 \bar{z}^2)$, where $\omega_x \equiv \omega_0$, ω_y, and ω_z are the angular frequencies in the x, y and z directions, respectively, and $\mathbf{r} \equiv (\bar{x}, \bar{y}, \bar{z})$ is the radial vector. The wave function can be written as $\Psi(\mathbf{r}; \tau) = \psi(\bar{x}, \bar{y}, \bar{z}, \tau)$. After a transformation of variables to dimensionless quantities defined by $x = \sqrt{2}\bar{x}/l$, $y = \sqrt{2}\bar{y}/l$, $z = \sqrt{2}\bar{z}/l$, $t = \tau\omega_0$, $l \equiv \sqrt{(\hbar/m\omega_0)}$ and $\phi(x, y, z, t) = \psi(\bar{x}, \bar{y}, \bar{z}, \tau)(l^3/\sqrt{8})^{1/2}$, the GP equation becomes

$$\left[-\frac{\partial^2}{\partial x^2} - \frac{\partial^2}{\partial y^2} - \frac{\partial^2}{\partial z^2} + \frac{x^2 + \kappa^2 y^2 + \nu^2 z^2}{4} + \mathcal{N} |\phi(x, y, z, t)|^2 - i\frac{\partial}{\partial t} \right] \phi(x, y, z, t) = 0, \quad (2.1)$$

where $\mathcal{N} = 8\sqrt{2}\pi n$, $\kappa = \omega_y/\omega_0$ and $\nu = \omega_z/\omega_0$ with nonlinearity $n = N_0 a/l$. The normalization condition for the wave function is

$$\int_{-\infty}^{\infty} dx \int_{-\infty}^{\infty} dy \int_{-\infty}^{\infty} dz |\phi(x, y, z, t)|^2 = 1. \quad (2.2)$$

3. Numerical Methods

3.1. Pseudospectral Runge-Kutta (PSRK) method

First we describe the PSRK method [16, 17] for the one-dimensional GP equation in some detail and then indicate the necessary changes for the three-dimensional case. The one-dimensional GP equation is obtained by eliminating kinetic energy (derivative) terms in y and z, setting $\kappa = \nu = 0$ and eliminating the y and z dependence of ϕ in (2.1), e.g.,

$$\left[-\frac{\partial^2}{\partial x^2} + \frac{x^2}{4} + \mathcal{N} |\phi(x,t)|^2 - i\frac{\partial}{\partial t} \right] \phi(x,t) = 0, \tag{3.1}$$

with the normalization $\int_{-\infty}^{\infty} dx |\phi(x,t)|^2 = 1$.

In this method the unknown function $\phi(x,t) \equiv \phi(x)$ is expanded in terms of a set of N known interpolating orthogonal functions $\{f_j(x)\}_{j=0}^{N-1}$ as follows [16]

$$\phi(x) \approx p_{N-1}(x) = \sum_{j=0}^{N-1} \frac{\alpha(x)}{\alpha(x_j)} f_j(x)\phi_j, \tag{3.2}$$

where $\{x_j\}_{j=0}^{N-1}$ is a set of distinct interpolation nodes, $\phi_j \equiv \phi(x_j)$, $\alpha(x)$ is a weight function, and the functions $\{f_j(x)\}_{j=0}^{N-1}$ satisfy $f_j(x_k) = \delta_{jk}$ (the Kronecker delta) and involve orthogonal polynomials of degree $(N-1)$, so that $\phi(x_k) = p_{N-1}(x_k), k = 0, 1, ..., N-1$. In this work the interpolating functions $\{f_j(x)\}_{j=0}^{N-1}$ are the Hermite polynomials $H_j(x)$: $f_j(x) = H_j(x)$. However, one could use other polynomials, such as, Chebyshev, Laguerre, and Legendre. One could also consider a Fourier (spectral) expansion of the wave function in terms of periodic cosine and sine functions. The Hermite polynomials are the eigenfunctions of the linearized GP equation and hence already satisfy the boundary conditions of the wave function of the GP equation [3]. Consequently, by choosing the Hermite polynomials in the expansion, (3.2) satisfies the proper boundary conditions by construction.

For obtaining the numerical solution, the GP equation (3.1) is defined and solved on the set of grid points x_j. The solution at any other point is obtained by using the interpolation formula (3.2), or any other convenient interpolation rule. The advantage of the expansion (3.2) is that when it is substituted in the GP equation, the space derivatives operate only on the known analytic functions $\alpha(x)$ and $f_j(x)$, so that one can define a matrix for the second-order space derivative [16]:

$$D_{k,j}^2 = \frac{d^2}{dx^2} \left[\frac{\alpha(x)}{\alpha(x_j)} f_j(x) \right]_{x=x_k}, \tag{3.3}$$

and the numerical differentiation process may therefore be performed as the matrix-vector product: $\sum_{j=0}^{N-1} D_{k,j}^2 \phi_j$. Consequently, the partial differential equation (3.1) is reduced to a set of coupled ODEs in the time variable t involving $\phi_j, j = 0, 1, ..., (N-1)$. In this way we obtain a set of ODEs by considering the original equations on a suitable set of discretization points (the roots of Hermite polynomials). One could have also used a Galerkin procedure [12] and projected the equations, essentially by integrating them against Hermite polynomials for that purpose. However, we do not explore this possibility in this paper.

For solving the set of ODEs we use the adaptive step-size control based on the embedded Runge-Kutta formulas due to Fehlberg [20], which gives a definite clue about

how to modify the step size in order to achieve a desired accuracy in a controlled way. For orders M higher than four of the Runge-Kutta formula, evaluation of more than M functions (though never more than $M+2$) is required. This makes the classic fourth order method requiring the evaluation of four functions more economic. Fehlberg suggested a fourth-order and a fifth-order method each requiring the evaluation of six functions. The difference between the results of these two gives the error δ in the fourth-order method with a step size h, where δ scales as $h^5 : \delta \propto h^5$. This scaling immediately gives the factor by which the step size h should be reduced, so that a desired δ can be obtained. The detailed fourth-order and fifth-order Runge-Kutta formulas of Fehlberg are given in [20]. We use these formulas with the constants given by Cash and Karp also tabulated in [20]. For the present problem we find that the use of Cash-Karp constants in the Fehlberg formulas leads to more accurate results than the original constants due to Fehlberg.

Next we specialize to the case of Hermite polynomials used to generate the solution. Hermite polynomials are very convenient in this case [25] as the solutions of the linear GP equation (3.1) with $\mathcal{N} = 0$ are Gaussian-type functions. They also satisfy the correct boundary conditions of the wave functions. In this case x_j are the roots of $H_{N-1}(x)$: $H_{N-1}(x_j) = 0, j = 0, 1, ..., N-1$. The roots can be found by diagonalizing a tridiagonal symmetric Jacobi matrix as described in [16] or otherwise. The weight functions are taken as $\alpha(x) = \exp(-x^2/2)$, such that expansion (3.2) becomes

$$p_{N-1}(x) = \sum_{j=0}^{N-1} \frac{\exp(-x^2/2)}{\exp(-x_j^2/2)} f_j(x)\phi_j, \tag{3.4}$$

where $f_j(x)$ are taken as

$$f_j(x) = \frac{H_{N-1}(x)}{H'_{N-1}(x_j)(x - x_j)}, \tag{3.5}$$

where prime refers to derivative with respect to x. Consequently, the differentiation matrix can be obtained from

$$D_{k,j}^2 = \frac{1}{\alpha(x_j)H'_{N-1}(x_j)} \frac{d^2}{dx^2} \left[\frac{\exp(-x^2/2)H_{N-1}(x)}{(x - x_j)} \right]_{x=x_k} \tag{3.6}$$

and calculated using an algorithm described in [16].

Using the differentiation matrix (3.6), the GP equation is discretized. The grid points are the roots of the Hermite polynomial $H_{N-1}(x_j) = 0$. However, the actual x_j values employed are obtained by scaling these roots by a constant factor so that most of the roots fall in the region where the condensate wave function is sizable and only a few points are located in the region where the wave function is negligible. For the spherically symmetric case $\omega_0 = \omega_y = \omega_z$, the discretization mesh in the three directions are identical. For the anisotropic cases, in general, the discretization points in the three directions are different from each other.

Though the passage from the one-dimensional to three-dimensional PSRK method is formally straightforward, it involves nontrivial computational steps. The unknown function $\phi(x, y, z, t) \equiv \phi(x, y, z)$ is expanded in terms of a set of N known interpolating orthogonal functions $\{f_j(x)\}_{j=0}^{N-1}$ as follows [16]

$$\phi(x, y, z) \approx p_{N-1}(x, y, z) = \sum_{i=0}^{N-1} \sum_{j=0}^{N-1} \sum_{k=0}^{N-1} \frac{\alpha(x)}{\alpha(x_i)} \frac{\alpha(y)}{\alpha(y_j)} \frac{\alpha(z)}{\alpha(z_k)} f_i(x) f_j(y) f_k(z) \phi_{ijk}, \tag{3.7}$$

where $\{x_j\}_{j=0}^{N-1}$ is a set of distinct interpolation nodes, $\phi_{ijk} \equiv \phi(x_i, x_j, x_k)$, and the functions α and f are defined as in the one-dimensional case, so that $\phi(x_i, y_j, z_k) = p_{N-1}(x_i, y_j, z_k)$. The differentiation matrices along x, y and z directions can be defined via (3.6) as in the one-dimensional case. Consequently, the partial differential GP equation (2.1) in three space variables is transformed to a set of ODEs in time variable on the grid points x_i, y_j and z_k, which is solved by the adaptive step-size controlled Runge-Kutta method. The wave function at any point is then calculated using the interpolation formula (3.7).

3.2. Finite-difference Crank-Nicholson (FDCN) method

The GP equation (2.1) has the form of the following nonlinear Schrödinger equation

$$i\frac{\partial\phi}{\partial t} = H\phi, \tag{3.8}$$

where the Hamiltonian H contains the different linear and nonlinear terms including the spatial derivatives. We solve this equation by time iteration after discretization in space and time using the finite difference scheme [18, 19, 8]. This procedure leads to a set of algebraic equations. In the present split-step method the iteration is conveniently performed in four steps by breaking up the full Hamiltonian into different derivative and nonderivative parts: $H = H_1 + H_2 + H_3 + H_4$, where

$$H_1 = \frac{x^2 + \kappa^2 y^2 + \nu^2 z^2}{4} + \mathcal{N}|\phi(x, y, z, t)|^2, \tag{3.9}$$

$$H_2 = -\frac{\partial^2}{\partial x^2}, \quad H_3 = -\frac{\partial^2}{\partial y^2}, \quad H_4 = -\frac{\partial^2}{\partial z^2}. \tag{3.10}$$

The time variable is discretized as $t_n = n\Delta$ where Δ is the time step. The solution is advanced first over the time step Δ at t_n by solving (3.8) with $H = H_1$ to produce an intermediate solution $\phi^{n+1/4}$ from ϕ^n, where ϕ^n is the discretized wave function at t_n. This propagation is performed essentially exactly for small Δ via

$$\phi^{n+1/4} = \mathcal{O}_{\mathrm{nd}}(H_1)\phi^n \equiv \exp(-i\Delta H_1)\phi^n, \tag{3.11}$$

where $\mathcal{O}_{\mathrm{nd}}(H_1)$ denotes time evolution with H_1 and the suffix 'nd' refers to non-derivative terms. Next we perform the time propagation corresponding to the operators $H_i, i = 2, 3, 4$ successively via the following semi-implicit Crank-Nicholson schemes [8]:

$$\phi^{n+2/4} = \mathcal{O}_{\mathrm{CN}}(H_2)\phi^{n+1/4} \equiv \frac{1 - i\Delta H_2/2}{1 + i\Delta H_2/2}\phi^{n+1/4} \tag{3.12}$$

$$\phi^{n+3/4} = \mathcal{O}_{\mathrm{CN}}(H_3)\phi^{n+2/4} \equiv \frac{1 - i\Delta H_3/2}{1 + i\Delta H_3/2}\phi^{n+2/4} \tag{3.13}$$

$$\phi^{n+1} = \mathcal{O}_{\mathrm{CN}}(H_4)\phi^{n+3/4} \equiv \frac{1 - i\Delta H_4/2}{1 + i\Delta H_4/2}\phi^{n+3/4}, \tag{3.14}$$

where $\mathcal{O}_{\mathrm{CN}}(H_i)$ denotes time evolution with H_i and the suffix 'CN' refers to Crank-Nicholson. Hence the final solution at time t_{n+1} is obtained from

$$\phi^{n+1} = \mathcal{O}_{\mathrm{CN}}(H_4)\mathcal{O}_{\mathrm{CN}}(H_3)\mathcal{O}_{\mathrm{CN}}(H_2)\mathcal{O}_{\mathrm{nd}}(H_1)\phi^n. \tag{3.15}$$

The details of the Crank-Nicholson discretization scheme can be found in [8]. The advantages of the above split-step method are the following. First, the error involved

in splitting the Hamiltonian is proportional to Δ^2 and can be neglected for small Δ. A considerable fraction H_1 of the Hamiltonian is treated fairly accurately without mixing with the Crank-Nicholson propagation. This method can deal with a large nonlinear term accurately and lead to stable and accurate converged result.

3.3. Calculational Details

In both the FDCN and PSRK methods the time iteration is started with the following normalized ground-state solution of the linear GP equation (2.1) with $\mathcal{N} = 0$:

$$\phi(x, y, z) = \left[\frac{\kappa\nu}{8\pi^3}\right]^{1/4} \exp\left[-(x^2 + \kappa y^2 + \nu z^2)/4\right]. \tag{3.16}$$

The norm of the wave function is conserved after each iteration due to the unitarity of the time evolution operator. However, it is of advantage to reinforce numerically the proper normalization of the wave function after several (100) time iterations in order to improve the precision of the result. Typical time step employed in the calculation is $\Delta = 0.001$. During the iteration the coefficient $n = N_0 a/l$ of the nonlinear term is increased from 0 at each step by $\Delta_1 = 0.001$ until the final value of nonlinearity n is attained. This corresponds to the final solution. Then several thousand time iterations of the equation were performed until a stable result is obtained.

For large nonlinearity, the Thomas-Fermi (TF) solution of the GP equation is a better approximation to the exact result [2] than the harmonic oscillator solution (3.16). In that case it might be advisable to use the TF solution as the initial trial input to the GP equation with full nonlinearity and consider time iteration of this equation without changing the nonlinearity. This time iteration is to be continued until a converged solution is obtained. However, in all the calculations reported in this paper only (3.16) is used as trial input. The use of initial TF solution did not lead to satisfactory result.

4. Numerical Results with the PSRK Method

4.1. Wave Function and Energy

The present method relies on time evolution and is suitable for both stationary and time-evolution problems. The stationary problems are governed by a wave function with trivial time dependence $\phi(x, y, z, t) = \phi(x, y, z) \exp(-i\mu t)$, where μ is a real energy parameter. Thus the stationary wave function ϕ and the parametric energy μ (the chemical potential) can be extracted from the evolution of the time-dependent GP equation over a macroscopic interval of time [4, 5]. Here we present results for the chemical potential of several BECs in three dimensions for spherically symmetric, axially symmetric and anisotropic cases. These traps with different geometries for ^{23}Na have been employed in experiments as well as in a time-independent solution of the three-dimensional GP equation [9]. The completely anisotropic trap employs the parameters $\omega_0^A = 354\pi$ rad/s, $\kappa = \sqrt{2}, \nu = 2$ as in the experiment of Kozuma *et al.* [15]. The cylindrically symmetric trap parameters are $\omega_0^C = 33.86\pi$ rad/s, $\kappa = \nu = 13.585$ as in [26]. The spherically symmetric trap parameters are $\omega_0^S = 87$ rad/s, $\kappa = \nu = 1$ [27]. We employ the scattering length of $a = 52a_0$ of Na, where a_0 is the Bohr radius [2].

In all calculations reported in this section we used 21 Hermite polynomials each in x, y and z directions so that we shall be dealing with a wave function in the form of

Table 1. The chemical potential μ corresponding to spherical, cylindrical and anisotropical geometries, respectively, for various numbers of condensate atoms $N_0 = 2^q$: present (†), reference [9] (‡).

q	Spherical			Cylindrical			Anisotropical		
	n	μ†	μ‡	n	μ†	μ‡	n	μ†	μ‡
10	0.50	1.82	1.825	0.55	17.39	17.384	1.77	3.55	3.572
11	1.00	2.05	2.065	1.10	19.32	19.392	3.54	4.32	4.345
12	1.98	2.42	2.435	2.19	22.27	22.359	7.09	5.39	5.425
13	3.97	2.95	2.970	4.38	26.66	26.620	14.18	6.86	6.904
14	7.93	3.69	3.719	8.77	32.41	32.682	28.35	8.83	8.900
15	15.86	4.71	4.743	17.54	41.61	41.055	56.70	11.55	11.572

a cubic array of dimension $21 \times 21 \times 21$. The maxima of x, y and z in discretization were chosen consistent with the trap parameters. Typical maxima $|x|_{\max}$, $|y|_{\max}$, and $|z|_{\max}$ are of the order of 8 for the spherical and anisotropical cases, although a smaller $|y|_{\max}$ and $|z|_{\max}$ (~ 3) together with a larger $|x|_{\max}$ (~ 10) have been used in the axially symmetric case because of large distortion of trap parameters in that case ($\kappa = \nu = 13.585$).

In table 1 we list the chemical potentials for different symmetries obtained from the PSRK approach as a function of number of atoms $N_0 = 2^q$ in the condensate and compare them with those of a calculation based on a discrete variable representation of the time-independent GP equation [9]. In the present calculation the chemical potentials are extracted from results of time evolution of the GP equation. The results were evaluated at a space point near the center of the BEC and averaged over several samples of calculation. The error (standard deviation) of the time averaged chemical potential is typically of the order of 0.2%. Considering that the present approach is based on time evolution, the precision is quite satisfactory − about less than a percentage point of discrepancy when compared to results of [9]. It was most difficult to obtain good convergence in the cylindrical case with highly distorted trap ($\kappa = \nu = 13.585$). A more carefully chosen values of the maxima $|x|_{\max}$ (~ 10), and $|y|_{\max} = |z|_{\max}$ (~ 3) were needed in this case.

In the following we study the convergence of the PSRK method in the anisotropical case with $q = 12$ calculated with $|x|_{\max} = 9$, $|y|_{\max} = 6.5$ and $|z|_{\max} = 5$ which seems to be optimal and were found after some experimentation. These values were taken to be roughly five times the root mean square (rms) sizes $\langle x, y, z \rangle_{\mathrm{rms}}$ in the respective directions. Here we consider the convergence of these rms sizes. After the proper nonlinearity is introduced in the GP equation, if we continue to integrate using the Runge-Kutta ODE solver routine the wave function and the rms sizes fluctuate a little. This type of fluctuation is common to time stepping methods for a partial differential equation. To quantify this fluctuation we calculate the rms sizes over 250 successive samples generated after 20 time steps of 0.01 each in the Runge-Kutta ODE routine. This corresponds to a total time interval of $250 \times 20 \times 0.01$ or 50 units. Then we calculate the mean rms sizes and the standard deviations which we show in table 2 for different number of expansion points N in (3.2). The numerical error in the rms sizes is typically less than one percent for $N > 10$ and the convergence is quite satisfactory.

Table 2. The convergence of the rms sizes $\langle x, y, z \rangle_{\mathrm{rms}}$ calculated with the PSRK method for the anisotropical $q = 12$ case for various number of space discretization points N.

N	$\langle x \rangle_{\mathrm{rms}}$	$\langle y \rangle_{\mathrm{rms}}$	$\langle z \rangle_{\mathrm{rms}}$
7	1.767 ± 0.029	1.295 ± 0.028	0.981 ± 0.015
8	1.707 ± 0.025	1.277 ± 0.018	0.959 ± 0.015
9	1.654 ± 0.022	1.251 ± 0.010	0.957 ± 0.004
10	1.690 ± 0.015	1.257 ± 0.008	0.959 ± 0.006
11	1.701 ± 0.002	1.263 ± 0.005	0.960 ± 0.007
12	1.691 ± 0.015	1.263 ± 0.005	0.960 ± 0.007
13	1.689 ± 0.004	1.262 ± 0.012	0.961 ± 0.008
14	1.691 ± 0.003	1.262 ± 0.013	0.962 ± 0.008
15	1.693 ± 0.006	1.263 ± 0.013	0.961 ± 0.009
16	1.692 ± 0.005	1.263 ± 0.013	0.962 ± 0.009

Considering that we are solving a partial differential equation in four variables this error is small. It will be difficult to obtain similar precision in the FDCN method in this problem even with a significantly larger number of space discretization points ($N > 100$) in each direction. The FDCN method is no match to the PSRK method in this problem with a smooth potential. However, the FDCN method seems to be very suitable for a rapidly varying potential, such as the optical-lattice potential considered in section 5, which requires a large number of equally distributed spatial discretization points for a faithful reproduction of the potential. Although, the present PSRK method yields satisfactory result for the stationary problem, its main advantage lies in its ability to tackle time-dependent problems as we shall see in the following.

4.2. Resonance Dynamics

The appearance of a resonance in the oscillation of a BEC due to a periodic variation of the scattering length has been postulated recently in spherically [23] and axially symmetric traps [24]. Here we extend this investigation to the more realistic and complicated case of an anisotropic trap.

In the case of a damped classical oscillator under the action of an external periodic force a resonance appears when the frequency of the external force is equal to or a multiple of the natural frequency of oscillation of the system. The natural frequency of oscillation of a trapped three-dimensional BEC along a certain direction (x, y, or z) is twice the trapping frequency in that direction [8, 28]. For a trapped BEC subject to a nonlinear external force due to a periodic variation in the scattering length given by $n = n_0 \sin(\Omega t)$, in analogy with the damped classical oscillator a resonance in the oscillation of the BEC along a particular direction is expected when Ω equals the natural frequency of oscillation in that direction or a multiple of this frequency. In the present numerical study of the anisotropic case we find that this is indeed the case.

To investigate the phenomenon of resonance we solve (2.1) with $\mathcal{N} = 8\pi\sqrt{2}n_0 \sin(\Omega t)$ with $n_0 = 0.3$. Actually, n_0 has to be less than a critical value n_{crit} (~ 0.55) in order to avoid collapse for attractive interaction [2, 7]. The actual critical
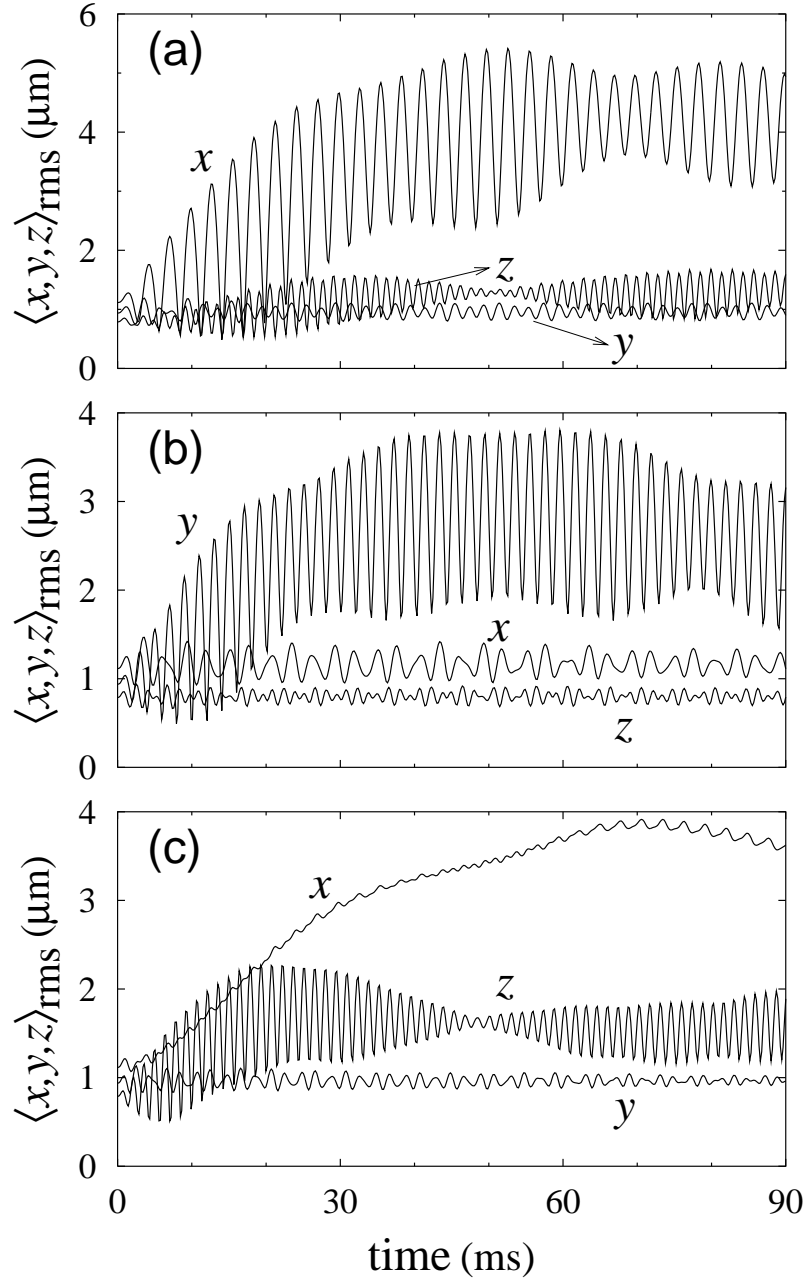
Figure 1. The rms sizes $\langle x \rangle_{\mathrm{rms}}$, $\langle y \rangle_{\mathrm{rms}}$, and $\langle z \rangle_{\mathrm{rms}}$ vs. time for a BEC in a harmonic trap with $\kappa = \sqrt{2}, \nu = 2$ subject to a sinusoidal variation of nonlinearity $n = 0.3[\sin(\Omega t)$ with (a) $\Omega = 2$, (b) $\Omega = 2\sqrt{2}$, and (c) $\Omega = 4$.

value depends on the asymmetry parameters κ and ν of the harmonic trap. For the spherically symmetric case $\kappa = \nu = 1$, $n_{\mathrm{crit}} = 0.575$ [2]. To study the resonance dynamics we use 31 Hermite polynomials in each of x, y, and z directions. The maximum values of $|x|$, $|y|$, and $|z|$ employed in space discretization are each 15. The resonance is best studied by plotting the rms sizes $\langle x, y, z \rangle_{\mathrm{rms}}$ vs. time. In this study we employ the trap parameters $\omega_x \equiv \omega_0 = 354\pi$ rad/s, $\kappa = \sqrt{2}$ and $\nu = 2$ [9, 15], so that the

unit of time is $\omega_0^{-1} = 0.9$ ms and of length is $l/\sqrt{2} = 1.115$ μm. For values of Ω off the resonance the rms sizes exhibit oscillation of very small amplitude. For resonance frequencies Ω, the rms sizes execute oscillation of large amplitude.

To illustrate the resonance we plot in figures 1 (a), (b), and (c) $\langle x, y, z \rangle_{\mathrm{rms}}$ vs. time for $\Omega = 2$, $2\sqrt{2}$, and 4, respectively. These values of Ω correspond to the natural frequency of oscillation of the condensate along the x, y, and z directions, respectively [8, 28]. In addition, $\Omega = 4$ is also twice the natural frequency of oscillation of the condensate along the x direction. So for $\Omega = 2$ and $2\sqrt{2}$ the rms values of x and y execute resonance oscillation as shown in figures 1 (a) and (b), respectively. At resonance in a particular direction, the corresponding dimension increases with time in a oscillatory fashion. The rms values of the other components do not show resonance. For $\Omega = 4$, rms values of both x and z exhibit resonance. In case of $\langle z \rangle_{\mathrm{rms}}$ this corresponds to the lowest harmonic and for $\langle x \rangle_{\mathrm{rms}}$ this corresponds to the first excited state. However, the behavior of $\langle x \rangle_{\mathrm{rms}}$ and $\langle z \rangle_{\mathrm{rms}}$ are different in this case.

5. Numerical Results with the FDCN Method

For a smooth trapping potential the PSRK method discussed in the last section yields excellent result with a smaller number of spatial discretization points which are unevenly distributed (at the scaled roots of the Hermite polynomial) compared to the FDCN method employing a relatively large number of evenly distributed spatial discretization points. For smooth potentials the CPU time in the PSRK method could be even an order of magnitude smaller than that in the FDCN method. However, the FDCN method has advantage in the case of a rapidly varying trapping potential requiring a large number of evenly distributed spatial discretization points for a proper description of the trapping potential. One such potential is the optical-lattice trapping potential recently used in BEC experiments in one [29] and three [30] dimensions.

The optical-lattice potential created with the standing-wave laser field of wavelength λ is given by $V_{\mathrm{opt}} = V_0 E_R \sum_{i=1}^{3} \sin^2(k_L x_i)$, with $E_R = \hbar^2 k_L^2/(2m)$, $k_L = 2\pi/\lambda$, and V_0 the dimensionless strength of the optical-lattice potential governed by the intensity of the laser [30]. In terms of the dimensionless laser wave length $\lambda_0 = \sqrt{2}\lambda/l$ and the dimensionless standing-wave energy parameter $E_R/(\hbar\omega) = 4\pi^2/\lambda_0^2$, V_{opt} is given by

$$\frac{V_{\mathrm{opt}}}{\hbar\omega} = V_0 \frac{4\pi^2}{\lambda_0^2} \sum_{i=1}^{3} \sin^2\left(\frac{2\pi}{\lambda_0}x_i\right). \tag{5.1}$$

In the actual experiment [30] this dimensionless standing-wave optical-lattice potential is superposed on the harmonic trapping potential of (2.1) and we present the solution of (2.1) under the action of spherically symmetric harmonic ($\kappa = \nu = 1$) as well as the optical-lattice potential (5.1).

To calculate the wave function we discretize the GP equation with time step 0.001 and space step 0.1 along x, y, and z directions spanning the cubic region $-4 < x, y, z < 4$. Consequently, the wave function is defined on a cubic array of dimension $80 \times 80 \times 80$. Starting the time iteration with the known harmonic oscillator solution for nonlinearity $n = 0$ and $V_0 = 0$, the nonlinearity n and the optical-lattice strength V_0 are slowly increased by equal amount in $1000n$ steps of time iteration until the desired values of n and V_0 are obtained. Then without changing any parameters the solution is iterated several thousand times so that a converged solution independent of the initial inputs
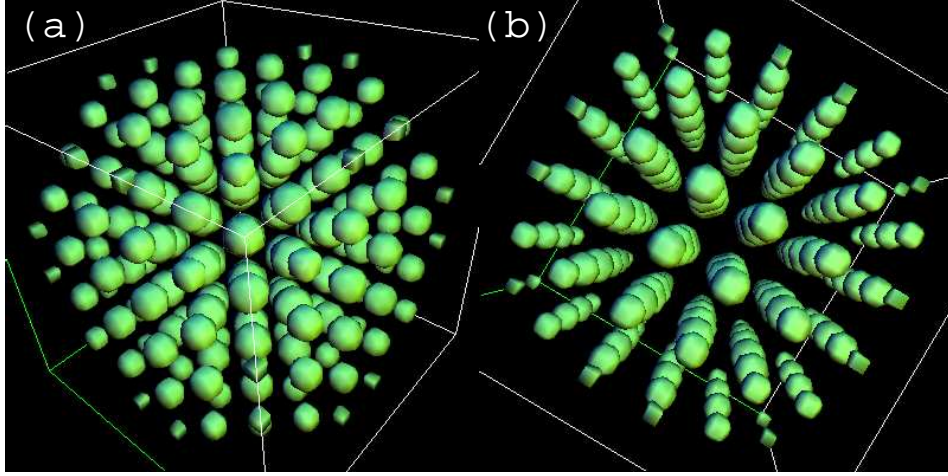
Figure 2. Three-dimensional contour plot of the interior part of the BEC ground state wave function under the combined action of the harmonic and the optical trap for $n \equiv N_0 a/l = 10$, $\lambda_0 = 1$ and $V_0 = 10$ on a cubic lattice of size $3 \times 3 \times 3$ ($-1.5 < x, y, z < 1.5$): (a) view along the diagonal of the cube and (b) along one of the axes of the cube.

is obtained. To illustrate the present method we calculate the wave function for the ground state for nonlinearity $n \equiv N_0 a/l = 10$, laser wave length $\lambda_0 = 1$ and optical-lattice strength $V_0 = 10$. Two views of the three-dimensional contour plot of the central part of the wave function on a cubic lattice of size $3 \times 3 \times 3$ are shown in figures 2 (a) and (b) as seen from two different angles. The droplets of BEC at each pit of the optical-lattice potential can be identified in figures 2. There are about 10 occupied cites in each of x, y, and z directions of which the central part is shown in figure 2.

6. Conclusion

In this paper we propose and implement a PSRK method [16] and contrast it with the FDCN method [8] for the numerical solution of the time-dependent nonlinear GP equation under the action of a three-dimensional trap by time iteration. In the PSRK method the unknown wave function is expanded in a set of known polynomials (Hermite). Consequently, the partial differential GP equation in three space and time variables becomes a set of coupled ODEs in time for the unknown coefficients, which is solved by a fourth-order adaptive step-size control Runge-Kutta method [20]. In the FDCN method the full Hamiltonian is split into the derivative and nonderivative parts. In this fashion the time propagation with the nonderivative parts can be treated very accurately. The time derivative part is treated by the Crank-Nicholson scheme in three independent steps. Both methods lead to stable and accurate results. The final result remains stable for thousands of time iteration of the GP equation.

We applied the PSRK method for the numerical study of certain stationary and time-evolution problems. We solved the GP equation for spherically symmetric, axially symmetric and anisotropic cases and calculated the chemical potential for different nonlinearities. The results compare well with those obtained by a time-independent approach [9]. The two sets of energy values agree to within a fraction of a percentage

point. The numerical error in the method is found to be less than one percent with a small number of expansion functions ($N \sim 20$). The PSRK method was also used to study the resonance dynamics of an anisotropic BEC under the action of periodic sinusoidal variation of the scattering length. When this period of oscillation coincides with the natural frequency of oscillation of the BEC along x, y, or z directions or a multiple thereof the corresponding rms size executes resonant oscillation [23, 24]. Using the FDCN method we study the ground state of a BEC under the combined action of a harmonic and a periodic optical-lattice trapping potential in three space dimensions.

The domain of applicability of the PSRK and FDCN methods seems to be complementary rather than overlapping. The PSRK method is more efficient and economic for smooth potentials where a relatively small number of expansion functions and unevenly distributed spatial discretization points seems to be adequate. The FDCN method employs a large number of evenly distributed spatial discretization points and is suitable for a rapidly varying potential, such as the optical-lattice potential, favoring such a distribution.

Acknowledgments

References

[1] Anderson M H, Ensher J R, Matthews M R, Wieman C E and Cornell E A 1995 *Science* **269** 198
Ensher J R, Jin D S, Matthews M R, Wieman C E and Cornell E A 1996 *Phys. Rev. Lett.* **77** 4984
Davis K B, Mewes M O, Andrews M R, van Druten N J, Durfee D S, Kurn D M and Ketterle W 1995 *Phys. Rev. Lett.* **75** 3969
Bradley C C, Sackett C A, Tolett J Jand and Hulet R G 1995 *Phys. Rev. Lett.* **75** 1687
Fried D G, Killian T C, Willmann L, Landhuis D, Moss S C, Kleppner D and Greytak T J 1998 *Phys. Rev. Lett.* **81** 3811
Pereira Dos Santos F, Léonard J, Junmin Wang, Barrelet C J, Perales F, Rasel E, Unnikrishnan C S, Leduc M and Cohen-Tannoudji C 2001 *Phys. Rev. Lett.* **86** 3459
Robert A, Sirjean O, Browaeys A, Poupard J, Nowak S, Boiron D, Westbrook C and Aspect A 2001 *Science 292* 461
Modugno G, Ferrari G, Roati G, Brecha R J, Simoni A and Inguscio M 2001 *Science 294* 1320
Weber T, Herbig J, Mark M, Naḡerl H-C and Grimm R *Science 299* 232
[2] Dalfovo F, Giorgini S, Pitaevskii L P and Stringari S 1999 *Rev. Mod. Phys.* **71** 463
[3] Edwards M and Burnett K 1995 *Phys. Rev. A* **51** 1382
Adhikari S K 2000 *Phys. Lett. A* **265** 91
[4] Ruprecht P A, Holland M J, Burnett K and Edwards M 1995 *Phys. Rev. A* **51** 4704
[5] Adhikari S K 2000 *Phys. Rev. E* **62** 2937
Adhikari S K 2001 *Phys. Rev. E* **63** 054502
[6] Dalfovo F and Stringari S 1996 *Phys. Rev. A* **53** 2477
Dalfovo F and Modugno M 2000 *Phys. Rev. A* **61** 023605
Holland M and Cooper J 1996 *Phys. Rev. A* **53** R1954
[7] Adhikari S K 2002 *Phys. Rev. E* **65** 016703
Adhikari S K 2002 *Phys. Rev. A* **65** 033616
[8] Adhikari S K and Muruganandam P 2002 *J. Phys. B: At. Mol. Phys.* **35** 2831
Adhikari S K and Muruganandam P 2003 *J. Phys. B: At. Mol. Phys.* **36** 409

[9] Schneider B I and Feder D L 1999 *Phys. Rev.* A **59** 2232

[10] Cerimele M M, Chiofalo M L, Pistella F, Succi S and Tosi M P 2000 *Phys. Rev.* E **62** 1382

[11] Reinhardt W P and Clark C W 1997 *J. Phys. B: At. Mol. Opt. Phys.* **30** L785
    Carr L D, Leung M A and Reinhardt W P 2000 *J. Phys. B: At. Mol. Opt. Phys.* **33** 3983
    Brand J and Reinhardt W P 2001 *J. Phys. B: At. Mol. Opt. Phys.* **34** L113
    Brand J and Reinhardt W P 2002 *Phys. Rev.* A **65** 043612

[12] Dion C M and Cances E 2002 *Preprint cond-mat/0209646*

[13] Bao W, Jaksch D and Markowich P A 2003 *Preprint cond-mat/0303239*
    Bao W and Du Q 2003 *Preprint cond-mat/0303241*
    Mottonen M, Mizushima T, Isoshima T, Salomaa M M and Machida K 2003 *Preprint cond-mat/0303256*

[14] Gross E P 1961 *Nuovo Cimento* **20** 454
    Pitaevskii L P 1961 *Zh. Eksp. Teor. Fiz.* **40** 646 (Engl. Transl. *Sov. Phys.-JETP* **13** 451)

[15] Kozuma M, Deng L, Hagley E W, Wen J, Lutwak R, Helmerson K, Rolston S L and Phillips W D 1999 *Phys. Rev. Lett.* **82** 871

[16] Weideman J A C and Reddy S C 2000 *ACM Transactions on Math Software* **26** 465

[17] Fornberg B 1996 *A Practical Guide to Pseudospectral Methods* (Cambridge: Cambridge University Press)

[18] Dautray R and Lions J -L 1993 *Mathematical Analysis and Numerical Methods for Science and Technology* vol 6 (Berlin: Springer-Verlag) p 46

[19] Koonin S E and Meredith D C 1990 *Computational Physics Fortran Version* (Reading: Addison-Wesley Pub. Co.) p 169

[20] Press W H, Flannery B P, Teukolsky S A and Vetterling W T 1993 *Numerical Recipes in Fortran 77: The Art of Scientific Computing* (Cambridge: Cambridge University Press)

[21] García-Ripoll J J, Pérez-García V M and Torres P 1999 *Phys. Rev. Lett.* **83** 1715
    Yukalov V I, Yukalova E P and Bagnato V S 1997 *Phys. Rev.* A **56** 4845
    Yukalov V I, Yukalova E P and Bagnato V S 2002 *Phys. Rev.* A **66** 043602

[22] Inouye S, Andrews M R, Stenger J, Miesner H -J, Stamper-Kurn D M and Ketterle W 1998 *Nature (London)* **392** 151

[23] Abdullaev F K, Bronski J C and Galimzyanov R M 2002 *Preprint cond-mat/0205464*

[24] Adhikari S K 2003 *J. Phys. B: At. Mol. Opt. Phys.* **36** 1109
    Adhikari S K 2003 *Phys. Lett.* A **308** 302

[25] Tang T 1993 *SIAM J. Sci. Comput.* **14** 59

[26] Stamper-Kurn D M, Miesner H -J, Inouye S, Andrews M R and Ketterle W 1998 *Phys. Rev. Lett.* **81** 500

[27] Hau L V, Busch B D, Liu C, Dutton Z Burns M M and Golovchenko J A 1998 *Phys. Rev.* A **58** R54

[28] Donley E A, Claussen N R, Cornish S L, Roberts J L, Cornell E A and Wieman C E 2001 *Nature (London)* **412** 295
    Santos L and Shlyapnikov G V 2002 *Phys. Rev.* A **66** 011602
    Saito H and Ueda M 2002 *Phys. Rev.* A **65** 033624
    Savage C M, Robins N P and Hope J J 2003 *Phys. Rev.* A **67** 014304
    Adhikari S K 2002 *Phys. Rev.* A **66** 013611
    Adhikari S K 2002 *Phys. Rev.* A **66** 043601

[29] Cataliotti F S, Burger S, Fort C, Maddaloni P, Minardi F, Trombettoni A, Smerzi A and Inguscio M 2001 Science **293** 843
    Pedri P, Pitaevskii L, Stringari S, Fort C, Burger S, Cataliotti F S, Maddaloni P, Minardi F and Inguscio M 2001 *Phys. Rev. Lett.* **87** 220401
    Adhikari S K 2003 *Eur. Phys. J.* D in press (*Preprint cond-mat/0208275*)

[30] M. Greiner M, Mandel O, Esslinger T, Hänsch T W and Bloch I 2002 *Nature (London)* **415** 39
    Adhikari S K and Muruganandam P 2003 *Phys. Lett.* A **310** 229
    Baizakov B B, Konotop V V and Salerno M 2002 *J. Phys. B: At. Mol. Phys.* **35** 5105